Mechanistic studies of the hydrolysis of *p*-nitrophenyl sulfate catalyzed by arylsulfatase from *Helix pomatia*

Iwona Stawoska[a]; Sylwia Gawęda[a]; Magdalena Bielak-Lakomska[a]; Małgorzata Brindell[a]; Krzysztof Lewiński[a]; Piotr Laidler[b]; Grażyna Stochel[a]

[a] Department of Inorganic Chemistry, Faculty of Chemistry, Jagiellonian University, Ingardena 3, 30-060 Kraków, Poland [b] Chair of Medical Biochemistry, Jagiellonian University, Medical College, Kopernika 7, 31-034 Kraków, Poland

PLEASE SCROLL DOWN FOR ARTICLE

Taylor & Francis
Taylor & Francis Group

Mechanistic studies of the hydrolysis of *p*-nitrophenyl sulfate catalyzed by arylsulfatase from *Helix pomatia*§

IWONA STAWOSKA†, SYLWIA GAWĘDA†,
MAGDALENA BIELAK-LAKOMSKA†,
MAŁGORZATA BRINDELL†, KRZYSZTOF LEWIŃSKI†,
PIOTR LAIDLER‡ and GRAŻYNA STOCHEL*†

†Department of Inorganic Chemistry, Faculty of Chemistry, Jagiellonian University,
Ingardena 3, 30-060 Kraków, Poland
‡Chair of Medical Biochemistry, Jagiellonian University, Medical College,
Kopernika 7, 31-034 Kraków, Poland

The kinetics of the hydrolysis of small aryl substrate *p*-nitrophenyl sulfate (*p*-NPS) catalyzed by arylsulfatase from *Helix pomatia* was studied at a wide range of temperatures as well as at ambient and elevated pressures. The employed kinetic assay techniques allow for the determination of activation entropy ($\Delta S^{\neq}$), activation enthalpy ($\Delta H^{\neq}$), as well as activation volume ($\Delta V^{\neq}$) which suggested associative interchange character of the sulfate ester hydrolysis. The pH dependence obtained for catalytic parameters suggests that two protonation/deprotonation reactions can occur and the optimum pH for the catalytic activity was also detected.

Keywords: Enzymatic hydrolysis; Arylsulfatase from *Helix Pomatia*; Activation volume; *p*-Nitrophenyl sulfate; Desulfatation mechanisms

1. Introduction

Sulfatases (EC 3.1.5.6) have been found in prokaryotic and eukaryotic organisms since the beginning of the twentieth century, but formerly their role was connected only to the degradation of organic sulfates in soils [1–3]. Interest in sulfatases rose significantly when it was discovered that sulfatase deficiencies in human organisms led to various types of lysosomal disorders. At least eight serious human diseases associated with the malfunction of single sulfatases have been described [4–6]. In addition, deficiency of all known sulfatases is a major reason of multiple sulfatase deficiency (MSD), a rare autosomal recessive disorder [7].

Sulfatases are a conserved family of enzymes, with sequence homology ranging from 20% to 60% and highly conserved *N*-terminal region carrying motif that is unique for this class of enzymes [8–10]. Arylsulfatases (ARSs) catalyze hydrolytic desulfatation

---

*Corresponding author. Email: stochel@chemia.uj.edu.pl
§On the occasion of Professor Rudi van Eldik's retirement.

of sulfate esters (CO–S) as well as sulfamates (CN–S) of various substrates, reactions (1) and (2), respectively.

$$ROSO_3^- + H_2O \rightarrow ROH + HSO_4^- \tag{1}$$

$$RN(H)SO_3^- + H_2O \rightarrow RNH_2 + HSO_4^- \tag{2}$$
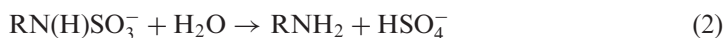
ARS from *Helix pomatia* (Roman snail) [9, 11] comprises 503 amino acids and shows 52% identity to human arylsulfatase B (HARSB) and 27% to human lysosomal arylsulfatase A (HARSA). The residues that are characteristic for the active site in eukaryotic ARSs are also present in the sequence of sulfatases from *H. pomatia*. Results obtained from crystallographic as well as mutagenesis studies of ARSs allowed detailed characterization of the structure of the active site, which is built by ten polar aminoacids and a divalent metal ion (table S1 and scheme S1) [9].

Mechanism of sulfatases activity became a subject of intense investigations when post-translational modification of cysteine (or serine in some prokaryotes) to formylglycine residue (FGly, 2-amino-3-oxypropanic acid, α-formylglycine) was proposed to play an important role in the hydrolysis reaction [10]. This modification has been found in all known sulfatases and it is now established well that this residue is crucial for the catalytic activity of the enzyme [12]. The crystal structure of HARSB determined by Bond *et al.* [13] gives an insight into the detailed structure of the active site as well as revealing its structural similarity to alkaline phosphatase (AP). This study allowed authors to propose an addition-hydrolysis mechanism of sulfate ester hydrolysis catalyzed by HARSB by referring to the mechanism suggested for phosphate ester hydrolysis catalyzed by AP [13]. The X-ray structure of HARSA, determined a year later by Lukatela *et al.* [14], showed that FGly can serve its catalytic functions only as a hydrated aldehyde. On the basis of this observation, the authors proposed a novel transesterification–elimination (TE) mechanism for this reaction [14, 15]. Many studies based on the crystal structure of HARS and proteinase-activated receptors (PARs), as well as mutagenesis of HARS, have been conducted in order to elucidate the single steps underlying the proposed mechanism (an excellent review on this subject is presented in reference [9], the original work includes references [14–19]). At present, it is believed that hydrolysis of sulfate ester occurs by TE mechanism as schematically shown in scheme 1. One of the hydrated groups of formylglycine begins a nucleophilic attack on the sulfur of the substrate leading to the release of conjugated alcohol and formation of a covalent FGly-sulfate intermediate (FGS). The final step comprises elimination of SO_4^{2-} and regeneration of FGly.

According to this mechanism, the configuration of the sulfate is inverted during hydrolysis since nucleophilic attack and elimination at the sulfate group occur from the same side [16]. The crystal structure of sulfatase from *Pseudomanas aeruginosa* (PARs) revealed that orientation of sulfate is optimal for nucleophilic attack of the FGly oxygen – $O\gamma1$ coordinated to the metal center and Asp317. At the same time, the oxygen – $O\gamma2$ coordinated to His115, Arg55, and Lys113 is crucial for the elimination of FGS to regenerate FGly [17]. In the studies where FGly was substituted by serine residue, the modified enzymes were not able to eliminate the sulfur group from FGS, confirming the importance of non-estrificated hydroxyl of the aldehyde hydrate in rapid desulfatation of substrate [18]. Evidence confirming the role of *gem*-diol came from the crystal structure of HARSA containing formylglycine phosphate derivative.
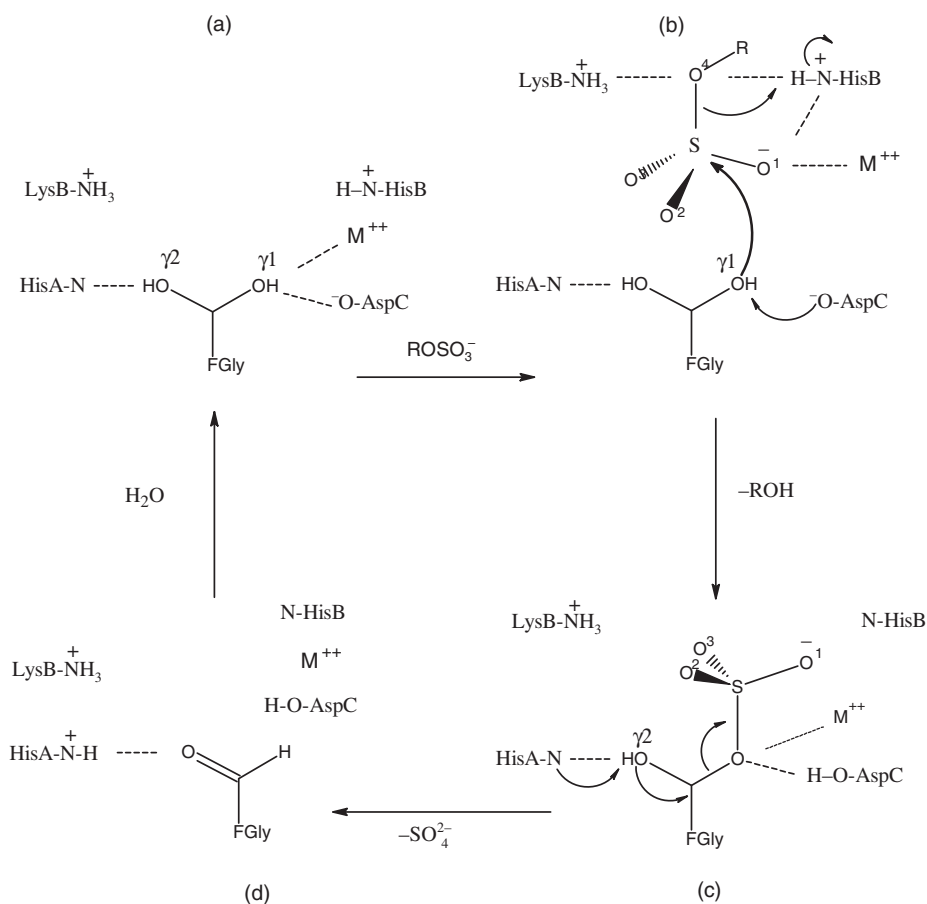
Scheme 1. A TE mechanism of catalytic activity of ARSs proposed on the basis of several independent studies [9, 14, 15].

The derivative, being a product of inhibition of ARS by phosphate esters, not only corresponds to one of the intermediates in the postulated mechanism but also shows that the enzyme has weak phosphate activity [19].

Whereas sulfatases have been a subject of many kinetic studies [20–27], details of TE mechanism still remain unclear. It is unknown whether a nucleophilic attack of oxygen $O\gamma1$ of FGly on the sulfur of substrate is preceded by release of RO^- of sulfate substrate according to a dissociative mechanism (D), scheme 2b, or release of RO^- is followed by bond formation between oxygen $O\gamma1$ and the sulfur of a substrate following an associative mechanism (A) (as proposed for phosphate esters [28]), scheme 2(a). Another possibility is simultaneous nucleophilic attack of the oxygen $O\gamma1$ at the sulfur of the substrate and release of RO^- in an interchange mechanism (I).

Studies of the mechanism of uncatalyzed sulfate ester hydrolysis, presented by Bourne *et al.* [29] and Hopkins *et al.* [30] have proved that the sulfur has mainly sulfur tricoordination in the transition state. However, results obtained by Hengge's group also for uncatalyzed reaction [7] revealed that the formation of a pentacoordinated intermediate is partially rate-determining, and the cleavage of the S–O bond takes place
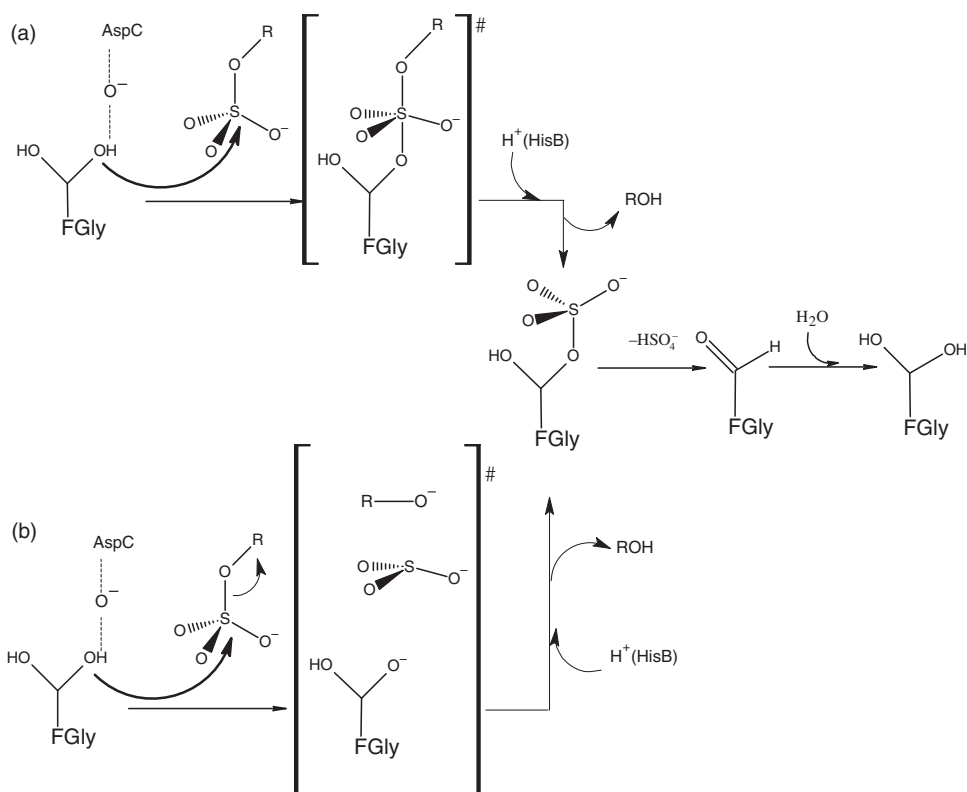
Scheme 2. Two extreme possible reaction pathways for hydrolysis of *p*-NPS catalyzed by ARS from *H. pomatia*. (a) An associative pathway with a five-coordinate sulfur in the transition state. (b) A dissociative pathway with tricoordinate sulfur in the transition state.

subsequently, which is an associative mechanism. Later, on the basis of [34]S isotope effect on sulfate ester hydrolysis as well as theoretical considerations, Burlingham *et al.* [31] proposed that cleavage of the S–O bond takes place during the rate-limiting step, pointing to a dissociative mechanism. The results obtained for uncatalyzed hydrolysis of sulfate ester could be helpful in explaining the reaction mechanism for catalytic reaction; however, due to the number of conflicting conclusions it appears not so straightforward. Therefore, more kinetic and stereochemical studies focusing on the catalyzed reaction are required to propose the reaction mechanism.

The results obtained for sulfate ester hydrolysis catalyzed by ARS from *Aspergillus oryzae* [16] indicate that the catalytic mechanism of sulfur transfer is stepwise with a covalent sulfoenzyme intermediate. Further mechanistic considerations are based on studies of *p*-nitrophenyl sulfate (*p*-NPS) hydrolysis catalyzed by ARS from *H. pomatia* and from *Aerobacter aerogenes* [22]. Their kinetic isotope effect (KIE) data obtained for ARS from *H. pomatia* revealed that in the transition state both S–O bond fission and protonation of the leaving group are far advanced, supportive for an associative or interchange mechanism. However, the leaving group KIE data obtained for ARS from *Aerobacter aerogenes* show that in the transition state protonation of the leaving group and S–O bond fission are not simultaneous (proton transfer lags behind S–O bond fission), indicating rather a dissociative mechanism.

In spite of many kinetic and stereochemical studies, the molecular nature of the transition state for sulfate ester hydrolysis catalyzed by ARSs is still not clear.

A useful approach to study the mechanisms of different types of reactions is application of kinetic methods using temperature and pressure as variables. By changing both temperature and pressure, it is possible to obtain the activation entropy ($\Delta S^{\neq}$), activation enthalpy ($\Delta H^{\neq}$), as well as volume of activation ($\Delta V^{\neq}$) which allows for the characterization of the transition state/states of the studied reaction. The pressure dependence of the equilibrium constant for binding of ligands allows determination of reaction volumes. Both reaction volumes and activation volumes provide unique information for determining the molecular mechanism of enzyme-catalyzed reaction.

Here we report the results of the studies on temperature and pressure effects on the hydrolysis of small aryl substrate, *p*-NPS catalyzed by ARS from *H. pomatia*. The employed kinetic assay techniques (continuous UV-Vis measurements in the wide range of temperatures as well as at ambient and elevated pressures) allow for the extraction of the appropriate rate and activation parameters. The obtained results are discussed in reference to the proposed reaction mechanism for hydrolysis of sulfate esters.

2. Experimental procedures

2.1. *Reagents*

The ARS from *H. pomatia* was purchased from ROCHE Applied Science and the activity of sulfatase was determined according to Baum's procedure [32]. The protein was stored at 4°C and in order to get active form it was dialysed against $1\,\mathrm{mmol\,L^{-1}}$ Tris/HCl, pH 7.4 containing $0.1\,\mathrm{mol\,L^{-1}}$ KCl. The enzyme was stable under such conditions for months [23]. Other reagents such as *p*-nitrocatechol sulfate (*p*-NCS), potassium *p*-NPS, and 2-amino-2-(hydroxymethyl)-1,3-propanediol (Tris) were obtained from Sigma–Aldrich. Solutions were prepared using deionized water purified by a Millipore system. All chemicals used throughout this study were of analytical reagent grade.

2.2. *UV-Vis measurements*

UV-Vis spectra at appropriate temperature were recorded in quartz cuvettes on a Shimadzu UV-2100 spectrophotometer equipped with a thermostated cell compartment CPS-260 ($\pm0.1^{\circ}$C). A pill-box cell combined with high-pressure equipment [33] was used to record UV-Vis spectra under elevated pressure (up to 160 MPa).

2.3. *Assay of ARS catalytic activity at ambient and elevated pressure*

In all kinetic measurements, the concentration of enzyme (arylosulfatase from *H. pomatia*) was kept constant ($8 \times 10^{-9}\,\mathrm{mol\,L^{-1}}$), while the concentration of substrate (*p*-NPS) was varied from 0.15 to $4.0\,\mathrm{mmol\,L^{-1}}$. Reactions were carried out in

Table 1. The V_{max} and K_m parameters obtained for the hydrolysis of *p*-NPS catalyzed by ARS from *H. pomatia*. Experimental conditions: $[ARS] = 8 \times 10^{-9} \, mol \, L^{-1}$, $[p\text{-NPS}] = (0.15 \times 10^{-3} \, to \, 4 \times 10^{-3}) \, mol \, L^{-1}$, $0.1 \, mol \, L^{-1}$ Tris/HCl, $T = 30°C$.

pH	$V_{max} \times 10^{-2}$ (mmol L^{-1} min^{-1})	K_m (mmol L^{-1})
8.68	2.57 ± 0.72	5.26 ± 1.58
8.08	5.42 ± 1.22	4.36 ± 1.06
7.43	3.38 ± 0.48	1.85 ± 0.32
7.08	2.06 ± 0.60	1.20 ± 0.43

$0.1 \, mmol \, L^{-1}$ Tris/HCl buffer at pH 7.4 (or other as described in table 1 for the experiments checking the pH effect on the reaction). The temperature effect on the investigated reaction was studied in the temperature range 15–35°C. The reaction was monitored spectrophotometrically by controlling *p*-nitrophenol (*p*-NP) release at 457 nm. The reported rate constants are mean values from at least five kinetic runs, and the quoted errors are based on standard deviations. The pressure effect on the catalytic process was studied at a constant temperature of 30°C using a stainless steel pressure chamber working at pressures up to 200 MPa. The reaction mixture (enzyme and substrate at the same concentration as used for temperature dependence measurement) was prepared at atmospheric pressure and room temperature. Experiments were performed in Tris/HCl buffer at pH 7.4 since the pK_a value of Tris is relatively insensitive to pressure up to 200 MPa [34]. After mixing of *p*-NSP with enzyme, the solution was placed into a pill-box cell, which was placed in the pressure chamber filled with thermostated water. The reaction mixture was equilibrated for 5–7 min prior to measurement. The velocity of *p*-NP formation was determined by measuring the absorbance changes at 457 nm. The reported rate constants are mean values from at least three kinetic runs, and the quoted errors are based on standard deviations. Further details of experimental conditions used in the presented experiments are specified in figure captions.

3. Results and discussion

3.1. *Steady state kinetics for enzyme-catalyzed hydrolysis of p-NPS*

Despite the fact that the hydrolytic activity of ARSs on various types of sulfate substrates has been studied since the early sixties, only a few results for ARS from *H. pomatia* and *p*-NPS as its substrate have been published [22, 23, 35, 36]. However, no pressure or temperature studies allowing for the determination of the activation parameters for this reaction were undertaken. Since the mechanism of nucleophilic substitution is not resolved, we decided to carry out detailed kinetic studies including both temperature and pressure measurements. Additional information gained from these studies could help in elucidation of the mechanism for enzymatic activity of ARSs. In order to find the best experimental conditions for pressure measurements, the hydrolysis of *p*-NPS catalyzed by ARS from *H. pomatia* was measured under different pH and temperature conditions. The UV-Vis spectrum of *p*-NPS in a neutral buffer
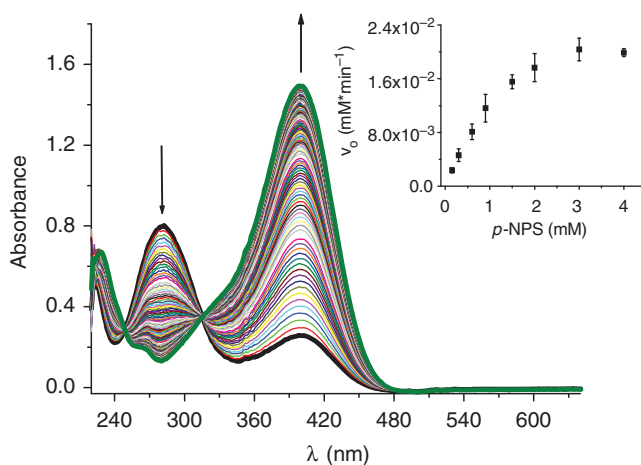
Figure 1. Representative UV-Vis spectral changes recorded for hydrolysis of *p*-NPS catalyzed by ARS from *H. pomatia*.
Experimental conditions: $[ARS] = 8 \times 10^{-9}\,mol\,L^{-1}$, $[p\text{-NPS}] = 1.5 \times 10^{-4}\,mol\,L^{-1}$, $0.1\,mol\,L^{-1}$ Tris/HCl buffer pH 7.4, $T = 25°C$.
Inset: Typical saturation plot of the reaction initial velocity (measured as the slopes of the kinetic traces obtained from absorbance changes recorded at $\lambda = 457\,nm$) as a function of substrate concentration.

exhibits a band with maximum absorbance at 282 nm. As can be seen in figure 1, the hydrolysis of *p*-NPS catalyzed by ARS from *H. Pomatia* leads to a decrease of this band and a new one at 400 nm, attributed to *p*-NP is formed. The enzyme activity was determined from the spectrophotometrical measurements by monitoring the changes in absorbance at $\lambda = 457\,nm$ which allow for the kinetic studies of all the chosen substrate concentrations.

On the basis of the hydrolysis of various sulfate substrates [18, 21, 24, 37] the process is characterized by Michaelis–Menten kinetics. Early theoretical considerations [38] as well as the mechanism of sulfatases activity proposed by Lukatela *et al.* [14] indicate that hydrolysis of small aryl sulfates can be described by a simple model, equation (3):

$$E + S \underset{k_{-1}}{\overset{k_1}{\rightleftharpoons}} ES \overset{k_2}{\longrightarrow} E + Y \tag{3}$$

where k_1 and k_{-1} are the rate constants for formation and dissociation of the enzyme-substrate complex, respectively ($K_d = k_{-1}/k_1$ is the dissociation constant), while k_2 is the rate constant for formation of the reaction product Y. Using the King–Altman method [39], assuming that reaction (3) is a cyclic process, the overall velocity equation can be written as follows:

$$v = \frac{dY}{dt} = \frac{k_1 k_2 [S]}{k_{-1} + k_2 + k_1 [S]}[E] \tag{4}$$

If the majority of the active sites of the enzyme are saturated by the substrate, k_2 equals k_{cat} and the maximal velocity V_{max} is defined as $k_{cat}[E_t]$, where $[E_t]$ denotes the total enzyme concentration. By defining the Michaelis constant as in equation (5):

$$K_m = \frac{k_2 + k_{-1}}{k_1} \tag{5}$$

Table 2. Catalytic properties of selected ARSs from various organisms.

Enzyme	Substrate	pH optimum	K_m (mmol L^{-1})	References
ARS A, human	*p*-NCS	5.5	0.4	[43]
		4.5	4.2	[45]
			3.5	[21]
ARS C, human	*p*-NPS	7.0	0.4	[41]
ARS C from Ox liver	*p*-NPS	7.9–8	2	[44]
	p-NCS	7.5	8	
ARS from digestive juice of *H. pomatia*	*p*-NPS	7.3–7.5	1.09	[23]
		~5	0.102	[22]
	p-NCS	7.2	2.3	
ARS from digestive juice/gland of *H. pomatia*	*p*-NPS	6–7.3	0.19–1.79	[35]
	p-NCS	6.5–7.5	0.03–1.25	
ARS from *A. aerogenes*	*p*-NPS	7.0	0.824	[22]
ARS from Alcaligenes metalcaligenes	*p*-NPS	8.8	0.47	[42]
	p–NCS	8.0	0.22	

the velocity equation derived from equation (4) can be converted to:

$$v = \frac{V_{max}}{\frac{K_m}{[S]} + 1} \tag{6}$$

For each investigated substrate concentration, the active sites of the enzyme were saturated as confirmed by the observation of the saturation plot of initial velocity *versus* *p*-NPS concentration (inset of figure 1). These findings give rise to the calculation of K_m and V_{max} parameters according to the standard procedure [40].

3.2. *The pH influence on the enzymatic activity of ARS from* H. pomatia

Examination of the influence of pH on *p*-NPS hydrolysis catalyzed by ARS from *H. pomatia* has shown a relatively strong effect of pH on maximal velocity of this reaction even in the narrow pH range (8.68–7.08), as described in table 1. The highest velocity can be obtained at pH 7.8–7.9, a little higher than values of optimum pH reported for other ARSs from *H. pomatia* (table 2). The differences are probably caused by variations in experimental conditions (e.g. temperature, buffer content) as well as in a source of the protein. Moreover, it is suggested that the optimum pH varies appreciably with the concentration of substrates [35] and enzyme [26]. For all types of ARSs, optimum pH for hydrolysis of *p*-NCS was lower than for *p*-NPS [21–23, 35, 41–45].

Studies of pH influence on catalytic parameters of *p*-NPS hydrolysis indicate that K_m increases with pH, which is in good agreement with previously published data [22, 23], whereas V_{max} increases with pH up to 7.9 (the optimum pH) followed by a rapid decrease (table 1). According to previous analysis [22], the dependence of $\log(V_{max}/K_m)$ *versus* pH has clearly bell-shaped profile (figure 2). Fitting these data to equation (7),

$$\log \frac{V_{max}}{K_m} = \log \frac{C}{1 + \frac{[H^+]}{K_{a_1}} + \frac{K_{a_2}}{[H^+]}} \tag{7}$$
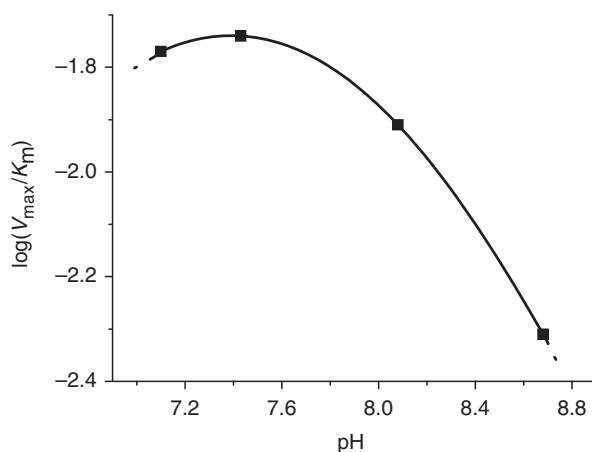
Figure 2.   The bell-shaped pH rate profile for hydrolysis of *p*-NPS catalyzed by ARS from *H. pomatia*. Experimental conditions: $[ARS] = 8 \times 10^{-9} \, \text{mol L}^{-1}$, $[p\text{-NPS}] = (0.15 \times 10^{-3}$ to $4 \times 10^{-3} \, \text{mol L}^{-1}$, $0.1 \, \text{mol L}^{-1}$ Tris/HCl buffer, $T = 30°C$.

Table 3. Kinetic parameters for the hydrolysis of *p*-NPS catalyzed by ARS from *H. pomatia*. Experimental conditions: $[ARS] = 8 \times 10^{-9} \, \text{mol L}^{-1}$, $[p\text{-NPS}] = (0.15 \times 10^{-3}$ to $4 \times 10^{-3}) \, \text{mol L}^{-1}$, $0.1 \, \text{mol L}^{-1}$ Tris/HCl buffer pH 7.4.

Pressure (MPa)	Temperature (K)	$V_{max} \times 10^{-2}$ (mmol L^{-1} min^{-1})	K_m (mmol L^{-1})	$k_{cat} \times 10^{3}$ (min^{-1})
0.1	288	2.06 ± 0.20	2.47 ± 0.18	2.57 ± 0.25
	290.5	2.01 ± 0.49	2.49 ± 0.52	2.51 ± 0.61
	293	2.21 ± 0.63	2.01 ± 0.47	2.77 ± 0.78
	295.5	2.79 ± 0.54	2.31 ± 0.32	3.48 ± 0.67
	298	2.71 ± 0.26	1.52 ± 0.11	3.38 ± 0.32
	303	3.58 ± 0.25	2.12 ± 0.12	4.47 ± 0.31
	308	4.36 ± 0.11	2.50 ± 0.55	5.45 ± 1.41
5	303	2.32 ± 0.70	1.60 ± 0.40	2.90 ± 0.87
40		2.23 ± 1.05	1.61 ± 0.63	2.79 ± 1.31
80		2.47 ± 1.17	1.62 ± 0.64	3.08 ± 1.46
120		1.95 ± 0.62	1.12 ± 0.27	2.43 ± 0.77
160		2.04 ± 0.91	0.82 ± 0.25	2.55 ± 1.14

can estimate pK_{a_1} (acidic limb) and pK_{a_2} (alkaline limb), equal 6.74 ± 0.28 and 8.04 ± 0.01, respectively. Our results together with those obtained by Gibby *et al.* [22] suggest that deprotonation of one diol group of the enzyme (pK_{a_1}) as well as protonation of the leaving group (pK_{a_2}) (scheme 2) occurs in the system.

3.3. *Temperature effect on K_m and V_{max}*

The kinetic behavior of *p*-NPS hydrolysis in buffered solution (pH 7.4) catalyzed by *H. pomatia* was studied in the temperature range 15–35°C. Systematic measurements of the maximal velocity, V_{max}, reveal the general tendency of this parameter to increase with temperature (table 3). Thus, the catalytic rate, k_{cat}, increases in a temperature range 15–35°C by a factor of two. A slightly different behavior was observed for K_m as
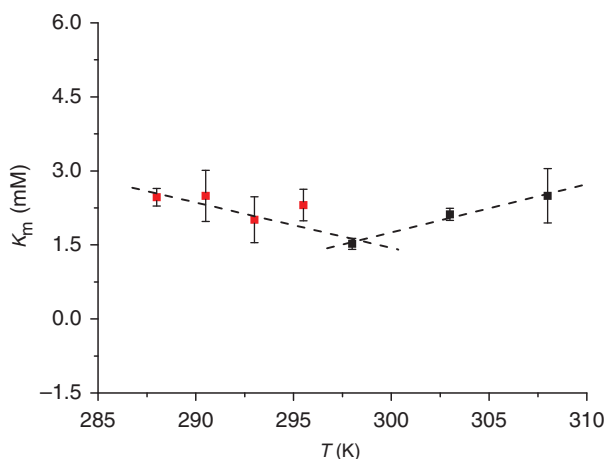
Figure 3. Temperature effect on the Michaelis constant, K_m, for *H. pomatia* ARS-catalyzed hydrolysis of *p*-NPS. Experimental conditions: $[ARS] = 8 \times 10^{-9} \, \text{mol L}^{-1}$, $[p\text{-NPS}] = (0.15 \times 10^{-3} \text{ to } 4 \times 10^{-3}) \, \text{mol L}^{-1}$, $0.1 \, \text{mol L}^{-1}$ Tris/HCl buffer pH 7.4, 15–35°C.

illustrated in figure 3. Since K_m is characterized by equation (5), it is possible to consider two cases: (1) if $k_2 \ll k_{-1}$, the dissociation of ES complex back to $E + S$ (equation 3) will be much faster than product formation and we can make an assumption that:

$$K_m = \frac{k_2 + k_{-1}}{k_1} \cong \frac{k_{-1}}{k_1} \cong K_d \tag{8}$$

where K_d is the dissociation constant of the ES complex. Taking into account that V_{max} increases with temperature, decrease of K_m in a temperature range from 15°C to 25°C suggests that k_2 has a minor contribution to K_m. Thus, under these conditions K_m is a measure of the affinity of the enzyme for the substrate; (2) if k_2 is comparable to k_{-1}, it is not possible to neglect k_2, as well as its participations in K_m value. The increase of the K_m value in a temperature range 25–35°C suggests faster product formation comparing to slower regeneration of the substrate.

In order to characterize the transition state, the activation parameters $\Delta H^{\neq}$ and $\Delta S^{\neq}$ were calculated according to the Eyring equation:

$$k = \frac{k_B T}{h} \exp\left(\frac{-\Delta G^{\neq}}{RT}\right) = \frac{k_B T}{h} \exp\left(\frac{-\Delta H^{\neq}}{RT}\right) \exp\left(\frac{\Delta S^{\neq}}{R}\right) \tag{9}$$

Catalytic rate constant, k_{cat}, was used to generate an Eyring plot of $\ln(k_{cat}/T)$ *versus* $1/T$ (figure 4) from which activation parameters were found and summarized in table 4. The parameters obtained for enzymatic hydrolysis of *p*-NPS are characterized by a positive activation enthalpy, $\Delta H^{\neq} = 28 \pm 2 \, \text{kJ mol}^{-1}$ and a negative value of activation entropy, $\Delta S^{\neq} = -83 \pm 10 \, \text{J mol}^{-1} \text{K}^{-1}$. The negative value of activation entropy suggests association or interchange rather than dissociation mechanism. Determination of $\Delta S^{\neq}$ in principle involves an extrapolation to $1/T$, which leads to differences in the $\Delta S^{\neq}$ values between different experiments apparently much larger than indicated by standard deviations for individual experiments. This discrepancy was the motivating factor for measuring the influence of pressure on the tested system.
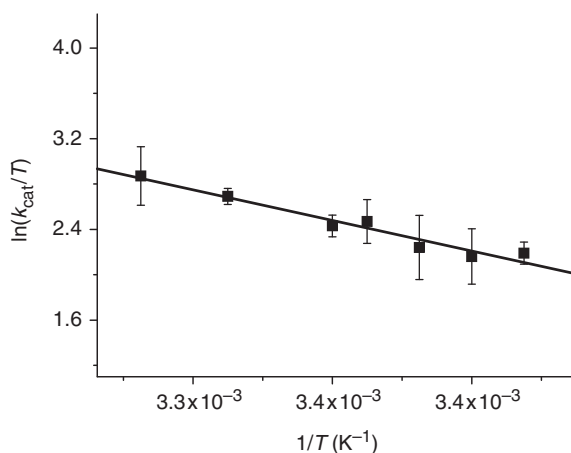
Figure 4. Eyring plot of $\ln(k_{cat}/T)$ *vs.* $1/T$ for hydrolysis of *p*-NPS catalyzed by ARS from *H. pomatia*. Experimental conditions: $[\text{ARS}] = 8 \times 10^{-9}\,\text{mol L}^{-1}$, $[p\text{-NPS}] = (0.15 \times 10^{-3}$ to $4 \times 10^{-3})\,\text{mol L}^{-1}$, $0.1\,\text{mol L}^{-1}$ Tris/HCl buffer pH 7.4.

Table 4. Kinetic and volumetric parameters for the hydrolysis of *p*-NPS catalyzed by ARS from *H. pomatia*.

Parameters	Values
$k_{cat} \times 10^3$ (min^{-1})	2.90 ± 0.87
$\Delta H^{\neq}$ (kJ mol^{-1})	28.04 ± 2.26
$\Delta S^{\neq}$ (J K^{-1} mol^{-1})	-83.06 ± 9.62
$\Delta V_{cat}^{\neq}$ (cm^3 mol^{-1})	2.5 ± 1.6
K_m independent of compressibility	
$\Delta V_b(1)$ (cm^3 mol^{-1})	0
$\Delta V_b(2)$ (cm^3 mol^{-1})	21.2 ± 0.8
$\Delta V_{obs}^{\neq}(A)$ (cm^3 mol^{-1})	$(-18.7^a \div 2.5^b)$
K_m dependent on compressibility	
$\Delta V_b(3)$ (cm^3 mol^{-1})	8.4 ± 5.1
$\Delta V_{obs}^{\neq}(B)$ (cm^3 mol^{-1})	$(-5.9^a \div 2.5^b)$
$\Delta \beta_{K_m}$ (cm^3 mol^{-1} MPa^{-1})	-0.23 ± 0.06

[a]Calculated for $[\text{S}] \ll K_m$.
[b]Calculated for $[\text{S}] \gg K_m$.

3.4. *Determination of binding and activation volumes*

Studies of enzyme-catalyzed hydrolysis of *p*-NPS under elevated pressure show dependence of the steady-state catalytic parameters, i.e. K_m, V_{max}, and k_{cat} on pressure. All data are presented in table 4. The pressure effect on catalytic parameters is described by equations (10) and (11):

$$\left(\frac{\partial \ln K_m}{\partial P}\right)_T = -\frac{\Delta V_b}{RT} \tag{10}$$

$$\left(\frac{\partial \ln k_{cat}}{\partial P}\right)_T = -\frac{\Delta V_{cat}^{\neq}}{RT} \tag{11}$$

In equation (10), ΔV_b is the volume change upon productive substrate binding. Since K_m can be regarded as a dissociation constant for productive bound substrate (b), $\Delta V_b = -\Delta V_{K_m}$ [46]. The $\Delta V_{cat}^{\neq}$ in equation (11) is the activation volume of the catalytic step. R denotes the gas constant ($8.314\,cm^3\,MPa\,mol^{-1}\,K^{-1}$) and T is the absolute temperature. The pressure dependence of K_m and k_{cat} can be described either by linear equations (12a) and (13a), respectively, or quadratic equations (12b) and (13b), respectively, which include compressibility effect [46].

$$\ln K_m = \ln K_{m,P_0} - \frac{\Delta V_{K_m}}{RT}P \tag{12a}$$

$$\ln K_m = \ln K_{m,P_0} - \frac{\Delta V_{K_m}}{RT}P + \frac{\Delta \beta_{K_m}}{2RT}P^2 \tag{12b}$$

$$\ln k_{cat} = \ln k_{0,P_0} - \frac{\Delta V_{cat}^{\neq}}{RT}P \tag{13a}$$

$$\ln k_{cat} = \ln k_{0,P_0} - \frac{\Delta V_{cat}^{\neq}}{RT}P + \frac{\Delta \beta_{cat}^{\neq}}{2RT}P^2 \tag{13b}$$

where $\Delta \beta_{cat}^{\neq}$ is the activation compressibility and $\Delta \beta_{K_m}$ is the compressibility changes upon substrate binding.

Applying the Michaelis–Menten model described by equation (4) and differentiation of the rate equation with respect to pressure give an expression for observed activation volume ($\Delta V_{obs}^{\neq}$) [46]:

$$\Delta V_{obs}^{\neq} = \Delta V_{k_{cat}}^{\neq} - \frac{\Delta V_b}{1 + \frac{[S]}{K_m}} \tag{14}$$

Equation 14 at two boundary conditions gives: for $[S] \ll K_m$, observed activation volume can be calculated as $\Delta V_{obs}^{\neq} = \Delta V_{k_{cat}}^{\neq} - \Delta V_b$ while for $[S] \gg K_m$, $\Delta V_{obs}^{\neq}$ is dominated by a contribution of $\Delta V_{k_{cat}}^{\neq}$. In the first approximation, the binding and activation volumes can be easily found from equations (12a) and (13a), respectively. However, there are at least three factors which influence linear dependence such as changes in: (1) quaternary structure and/or modification of the active site architecture, (2) a compressibility and (3) the rate-determining step which can occur under elevated pressure [46]. We have found that in the tested system, the dependence of $\ln k_{cat}$ *versus* pressure is linear (figure 5), allowing us to define $\Delta \beta_{cat}^{\neq}$ as zero for this enzyme. From equation (13a), we find that the catalytic activation volume has a value $2.5 \pm 1.6\,cm^3\,mol^{-1}$.

The obtained data for pressure effect on K_m can be discussed in two separate ways, since dependence of $\ln K_m$ *versus* pressure allows applying either linear (equation 12a) or quadratic equations (equation 12b). If we presume that K_m is independent of compressibility, $\Delta \beta_{K_m} = 0$ and the linear plots can be fitted (figure 6a). Since the pressure dependence of K_m is biphasic (figure 6a), the obtained data should be considered separately in two pressure ranges, ambient to 80 MPa, $\Delta V_b(1)$, and from 80 to 160 MPa, $\Delta V_b(2)$. The substrate binding to the active site seems not influenced by pressure lower than 80 MPa, for which $\Delta V_b(1) \cong 0$. Consequently, the observed activation volume $\Delta V_{obs}^{\neq}(A1) = \Delta V_{k_{cat}}^{\neq}$ and equals $2.5 \pm 1.6\,cm^3\,mol^{-1}$. Decrease of K_m
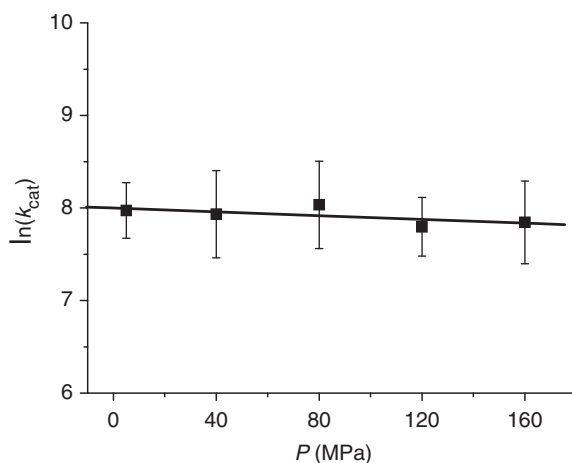
Figure 5. Plot of $\ln(k_{cat})$ *vs.* pressure for *p*-NPS hydrolysis catalyzed by ARS from *H. pomatia*. Experimental conditions: $[ARS] = 8 \times 10^{-9}$ mol L^{-1}, $[p\text{-NPS}] = (0.15 \times 10^{-3}$ to $4 \times 10^{-3})$ mol L^{-1}, 0.1 mol L^{-1} Tris/HCl buffer pH 7.4. Pressure range 5–160 MPa, $T = 30°C$.
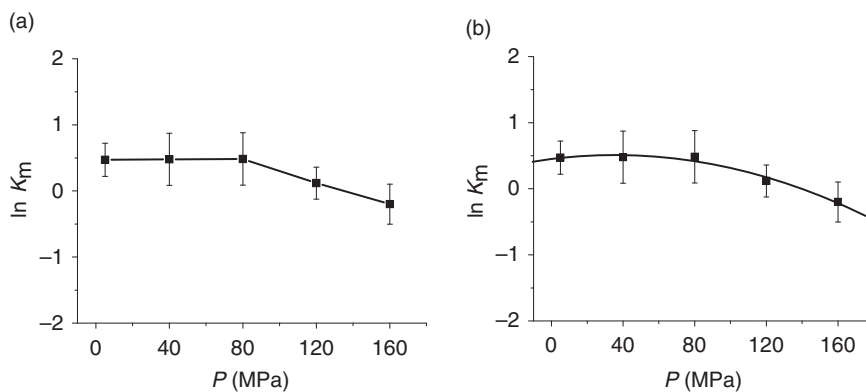

Figure 6. The dependence of $\ln K_m$ *vs.* pressure for *p*-NPS hydrolysis catalyzed by ARS from *H. pomatia* without (a) and with (b) the influence of compressibility changes upon substrate binding. Experimental conditions: $[ARS] = 8 \times 10^{-9}$ mol L^{-1}, $[p\text{-NPS}] = (0.15 \times 10^{-3}$ to $4 \times 10^{-3})$ mol L^{-1}, 0.1 mol L^{-1} Tris/HCl buffer pH 7.4. Pressure range 5–160 MPa, $T = 30°C$.

in a pressure range 80–160 MPa allowed us to calculate $\Delta V_b(2) = 21.2 \pm 0.8$ cm^3 mol^{-1}. In order to determine activation volume in this pressure range, it was necessary to take into account substrate concentration. For $[S] \ll K_m$, the minimal value of the activation volume can be found as $\Delta V_{obs}^{\neq}(A2_{min}) = -18.7$ cm^3 mol^{-1}, whereas for $[S] \gg K_m$, observed activation volume $\Delta V_{obs}^{\neq}(A2_{max}) = 2.5 \pm 0.8$ cm^3 mol^{-1} (table 4). Therefore, assuming independence of K_m from compressibility for the broad range of substrate concentration, the calculated values of the observed activation volume ($\Delta V_{obs}^{\neq}(A)$) varies from -18.7 to 2.5 cm^3 mol^{-1}.

Fitting a quadratic equation (12b) to the same data (figure 6b) allows for the calculation of $\Delta V_b(3)$, which was found to be 8.4 ± 5.1 cm^3 mol^{-1} as well as $\Delta \beta_{K_m}$ with

value of $-0.23 \pm 0.06\,\mathrm{cm^3\,mol^{-1}\,MPa^{-1}}$ (table 4). Considering a different substrate concentrations (see above), we calculated the observed activation volume $\Delta V_{\mathrm{obs}}^{\neq}(B)$ ranging from -5.9 to $2.5\,\mathrm{cm^3\,mol^{-1}}$ for $[S] \ll K_{\mathrm{m}}$ and $[S] \gg K_{\mathrm{m}}$, respectively. The decrease of activity may be an effect of modifications of enzyme conformation or changes of the substrate binding mechanism [47, 48].

Volume changes upon substrate binding (ΔV_{b}) both models (K_{m} independent and dependent on compressibility) are positive and some contribution to these values can originate from desolvation of substrate entering the active site [14]. Generally, the changes of activation volumes were negative for low substrate concentrations and close to zero (positive) for high substrate concentrations (table 4). The interpretation of obtained values is often ambiguous because experimental values are a sum of three components, as seen in equation (15).

$$\Delta V^{\neq} = \Delta V_{\mathrm{intr}}^{\neq} + \Delta V_{\mathrm{solv}}^{\neq} + \Delta V_{\mathrm{canf}}^{\neq} \tag{15}$$

where $\Delta V_{\mathrm{intr}}^{\neq}$ the intrinsic contribution, refers to formation and disruption of chemical bonds, $\Delta V_{\mathrm{solv}}^{\neq}$ is associated with the influence of water molecules on surrounding moieties, and $\Delta V_{\mathrm{canf}}^{\neq}$ shows the influence of conformational changes as a result of chemical reactions. Therefore, it is necessary to distinguish these three components in the obtained activation volume. As reported previously, solvation contribution for enzymatic reaction is usually dominant for overall activation volume [49]. Also in this case, water seems to play a key role, especially because it is engaged in the mechanism of enzymatic hydrolysis of *p*-NPS (scheme 2). $\Delta V_{\mathrm{intr}}^{\neq}$ depends on the character of bonds which are formed or broken during the reaction steps. For disruption of ester bonds this value was found to be around $+10\,\mathrm{cm^3\,mol^{-1}}$ [50]. The conformational contribution can usually be neglected, with the exception of oligomeric enzymes. Thus, if we assume independence of the system from compressibility changes upon substrate binding, we can calculate the solvation effect in a range of $\Delta V_{\mathrm{solv}}^{\neq}(1) = -7.5\,\mathrm{cm^3\,mol^{-1}}$ for the pressure up to $80\,\mathrm{MPa}$ and $\Delta V_{\mathrm{solv}}^{\neq}(2)$ from -7.5 to $-28.7\,\mathrm{cm^3\,mol^{-1}}$ at higher values of pressure. Accounting for the compressibility influence on K_{m} in the tested pressure range gives us the solvation contribution form -15.9 to $-8.5\,\mathrm{cm^3\,mol^{-1}}$. All the obtained values are negative in the range from *ca* -29 to $-8\,\mathrm{cm^3\,mol^{-1}}$ and in well agreement with values obtained for other enzymes [51].

4. Conclusions

We have obtained negative $\Delta S^{\neq}$, which could indicate the associative or associative interchange mechanism for hydrolysis of sulfate ester. The value of the observed activation volume ($\Delta V_{\mathrm{obs}}^{\neq}$), independent of whether it was calculated with an assumption that K_{m} depends on compressibility changes upon substrate binding or not, were found to be from close to zero positive ($2.5\,\mathrm{cm^3\,mol^{-1}}$) to negative ($-18.7\,\mathrm{cm^3\,mol^{-1}}$). The small positive value of catalytic activation volume ($2.5 \pm 1.6\,\mathrm{cm^3\,mol^{-1}}$) and rather big uncertainty suggest that pressure only slightly affects catalytic reaction rate. Based on both temperature and pressure influence on catalytic reaction rate (k_{cat}) and Michaelis constant (K_{m}), we suggest the associative interchange mechanism. In the transition state in which sulfur from sulfate substrate

has the character of five-coordinative species. The bond that is formed between incoming nucleophile and the sulfur is expected to be as strong as a bond between sulfur and the leaving groups.

In these studies, for the first time, activation parameters of *p*-NPS hydrolysis catalyzed by ARS from *H. pomatia* were determined. Results of kinetic measurements showed the influence of pressure on the mechanism. We discussed two separate ways of interpretation of the obtained results, which were already presented for different enzymatic systems [51, 52]. Considering independence of K_m from compressibility changes upon substrate binding, we suggest that in a pressure range up to 80 MPa, the system is characterized by an interchange mechanism of nucleophilic substitution. The slightly positive value of $\Delta V^{\neq}_{obs}$ implies that the sulfur in a transient product is three- rather than five-coordinate. Nevertheless, increase of pressure shifts this dependence to associative mechanism and strongly indicates a five-coordinate transient product. Taking into account the influence of $\Delta \beta_{K_m}$, we found confirmation of our conclusions concerning the type of mechanism of *p*-NPS hydrolysis catalyzed by ARS from *H. pomatia*.

Acknowledgment

References

[1] J.W. Fitzgerald. *Microbiol. Mol. Biol. Rev.*, **40**, 698 (1976).
[2] J.W. Fitzgerald, M.E. Watwood, F.A. Rose. *Soil Biol. Biochem.*, **17**, 885 (1985).
[3] G. Lou, P.R. Warman. *Biol. Fertil. Soils*, **14**, 112 (1992).
[4] E.F. Neufeld, J. Muenzer. *The Metabolic and Molecular Bases of Inherited Disease*, Vol. III, 8th Edn, McGraw-Hill, New York (1999).
[5] A. Ballabio, L.J. Shapiro. *The Metabolic and Molecular Bases of Inherited Disease*, Vol. III, 8th Edn, McGraw-Hill, New York (1999).
[6] K. von Figura, V. Gieselmann, J. Jaeken. *The Metabolic and Molecular Bases of Inherited Disease*, Vol. III, 8th Edn, McGraw-Hill, New York (1999).
[7] J.J. Hopwood, A. Ballabio. *The Metabolic and Molecular Bases of Inherited Disease*, Vol. III, 8th Edn, McGraw-Hill, New York (1999).
[8] B. Franco, G. Meroni, G. Parenti, J. Levilliers, L. Bernard, M. Gebbla, L. Cox, P. Maroteaux, L. Sheffeld, G.A. Rappold, G. Andria, C. Petit, A. Ballabio. *Cell*, **81**, 15 (1995).
[9] S.R. Hanson, M.D. Best, C.-H. Wong. *Angew. Chem. Int. Ed.*, **43**, 5736 (2004).
[10] B. Schmidt, T. Selmer, A. Ingendoh, K. von Figura. *Cell*, **82**, 271 (1995).
[11] U. Wittstock, M. Fischer, I. Svendsen, B.A. Halkier. *IUBMB Life*, **49**, 71 (2000).
[12] C. Marquordt, Q. Fang, E. WillDagger, J. Peng, K. von Figura, T. Dierks. *J. Biol. Chem.*, **278**, 2212 (2003).
[13] C.S. Bond, P.R. Clements, S.J. Ashby, C.A. Collyer, S.J. Harrop, J.J. Hopwood, J.M. Guss. *Structure*, **5**, 277 (1996).
[14] G. Lukatela, K. Krauss, K. Theis, T. Selmer, V. Gieselmann, K. von Figura, W. Saenger. *Biochemistry*, **37**, 3654 (1998).
[15] R. von Bulow, B. Schmid, T. Dierks, K. von Figura, I. Usón. *J. Mol. Biol.*, **305**, 269 (2001).
[16] C.L.L. Chai, W.A. Loughlin, G. Lowe. *Biochem. J.*, **287**, 805 (1992).
[17] I. Boltes, H. Czapinska, A. Kahnert, R. von Bulow, T. Dierks, B. Schmidt, K. von Figura, M.A. Kertesz, I. Uson. *Structure*, **9**, 483 (2001).
[18] M. Recksiek, T. Selmer, T. Dierks, B. Schmidt, K. von Figura. *J. Biol. Chem.*, **273**, 6096 (1998).

[19] M. Chruszcz, P. Laidler, M. Monkiewicz, E. Ortlund, L. Lebioda, K. Lewiński. *J. Inorg. Biochem.*, **96**, 386 (2003).
[20] J.S. Bruce, M.W. McLean, F.B. Williamson, W.F. Long. *Eur. J. Biochem.*, **152**, 72 (1985).
[21] A. Knaust, B. Schmidt, T. Dierks, R. von Bulow, K. von Figura. *Biochemistry*, **37**, 13941 (1998).
[22] S.G. Gibby, J.M. Younker, A.C. Hengge. *J. Phys. Org. Chem.*, **17**, 541 (2004).
[23] A.B. Roy, E.A. Williams. *Comp. Biochem. Physiol.*, **93B**, 229 (1989).
[24] A.A. Farooqui. *Arch. Int. Physiol. Biochim.*, **84**, 479 (1976).
[25] A.B. Roy. *Biochem. J.*, **55**, 653 (1953).
[26] G.D. Lee, R.L. van Etten. *Arch. Biochem. Biophys.*, **166**, 280 (1975).
[27] A.B. Roy, T.J. Mantle. *Biochem. J.*, **261**, 689 (1989).
[28] J.E. Coleman. *Annu. Rev. Biophys. Biomol. Struct.*, **21**, 441 (1992).
[29] N. Bourne, A. Hopkins, A. Williams. *J. Am. Chem. Soc.*, **107**, 4327 (1985).
[30] A. Hopkins, R.A. Day, A. Williams. *J. Am. Chem. Soc.*, **105**, 6062 (1983).
[31] B.T. Burlingham, L.M. Pratt, E.R. Davidson, V.J. Shiner, J. Fong, T.S. Widlanski. *J. Am. Chem. Soc.*, **125**, 13036 (2003).
[32] H. Baum, K.S. Dodgson, B. Spencer. *Clin. Chim. Acta*, **4**, 453 (1959).
[33] A.W. Spitzer, F. Gartig, R. van Eldik. *Rev. Sci. Instrum.*, **59**, 2092 (1988).
[34] R.C. Neuman Jr, W. Kauzmann, A. Zipp. *J. Phys. Chem.*, **77**, 2687 (1973).
[35] K.S. Dodgson, G.M. Powell. *Biochem. J.*, **73**, 666 (1959).
[36] P. Jarrige, R. Henry. *Bull. Soc. Chim. Biol.*, **34**, 872 (1952).
[37] A.L. Fluharty, R.L. Stevens, E.B. Goldstein, H. Kihara. *Biochim. Biophys. Acta*, **566**, 321 (1979).
[38] A.B. Roy. *Biochim. Biophys. Acta*, **276**, 475 (1972).
[39] R.A. Copeland. *Enzymes: A Practical Introduction to Structure, Mechanism, and Data Analysis*, VCH, New York (1996).
[40] A. Cornish-Bowden. *Fundamentals of Enzyme Kinetics*, 3rd reprint, revised Edn, Portland Press, London (2002).
[41] L. Dibbelt, E. Kuss. *Biol. Chem. Hoppe-Seyler*, **372**, 173 (1991).
[42] K.S. Dodgson, B. Spencer, K. Williams. *Biochem. J.*, **61**, 374 (1955).
[43] A.A. Farooqui, P. Mandel. *Biomedicine*, **26**, 232 (1977).
[44] A.B. Roy. *Biochem. J.*, **64**, 651 (1956).
[45] A. Waldow, B. Schmidt, T. Dierks, R. von Bulow, K. von Figura. *J. Biol. Chem.*, **274**, 12284 (1999).
[46] P. Masson, C. Balny. *Biochim. Biophys. Acta*, **1724**, 440 (2005).
[47] V.V. Mozhaev, K. Heremans, J. Frank, P. Masson, C. Balny. *Trends Biotechnol.*, **12**, 493 (1994).
[48] C.I. Branden, H. Jornvall, H. Eklund, B. Furugen. *Alcohol Dehydrogenase*, 3rd Edn, Academic Press, New York (1975).
[49] P. Masson, M.-T. Froment, S. Fort, F. Ribes, N. Bec, C. Balny, L.M. Schopfer. *Biochim. Biophys. Acta*, **1597**, 229 (2002).
[50] R. van Eldik, T. Asano, W.J. Le Noble. *Chem. Rev.*, **89**, 549 (1989).
[51] P. Masson, N. Bec, M.T. Froment, F. Nachon, C. Balny, O. Lockridge, L.M. Schopfer. *Eur. J. Biochem.*, **271**, 1980 (2004).
[52] S. Marchal, H.M. Girvan, A.C.F. Gorren, B. Mayer, A.W. Munro, C. Balny, R. Lange. *Biophys. J.*, **85**, 3303 (2003).